The Solar Probe Heatshield Development

J. E. Randolph, W. Imbriale, R. N. Miyake, - JPL-Caltech*
E. A. Pierson – Lockheed/Martin Astronautics**
R. B. Dirling, Jr. – Science Applications International Corporation***

ABSTRACT

A NASA mission that will travel close to the sun requires a unique heatshield to protect the spacecraft and the instruments from the peak flux of 400 W/cm^2 found at the mission's perihelion of 4 solar radii (~ 0.02 AU). The heatshield must be designed to minimize its mass loss while operating at over 2000 K at perihelion. An architectural characteristic of the spacecraft and mission design suggested that if the heatshield could have the shape of a paraboloidal shell, it could also function as an off-axis high gain antenna for X-band communications at perihelion. The main shell of the shield consists of a high density carbon-carbon material with a thickness of about one millimeter that forms a paraboloidal structure having an "elliptical" planform with about 2 m by 3 m axes. Following an extensive testing program to screen various carbon-carbon shield materials, a candidate material has been chosen that promises to have optical properties that would minimize the operating temperature at the high solar fluxes, thereby minimizing the mass loss at these high temperatures. The testing program confirmed the desired characteristics of this carbon-carbon shield material and a specific material was selected for the shield. The material is fabricated with a densification process using chemical vapor infiltration (CVI). A final chemical vapor deposition (CVD) process produces a pyrolytic graphite coating to minimize the absorptivity/emissivity ratio at high temperatures. No additional coatings will be necessary to satisfy the design requirements. The CVD process also promises to minimize the mass loss (sublimation) at these operating temperatures. The RF reflectivity of the material at the X-band frequency (~ 8 GHz) is sufficient to allow the shield to operate well as an antenna at over 2000 K. The paper will describe the history of the shield development, the materials fabrication processes, the materials selection process, and the shield design concept that is in the current Solar Probe design.

---

* JPL-Caltech, 4800 Oak Grove Dr., Pasadena, CA 91109, (818) 354-2732, FAX (818) 393-9815, jrandolph@jpl.nasa.gov

** Lockheed Martin Astronautics, P. O. Box 179, Denver, CO 80201, (303) 971-9109, edward.a.pierson@lmco.com

*** Science Applications International Corp., 18350 Mt. Langley St., Fountain Valley, CA 92708, (714) 963-7476, dirlingr@saic.com

1. INTRODUCTION

The destination of the Solar Probe is the atmosphere of the sun. It will approach the Sun within 2 million kilometers of the surface (a perihelion radius of 4 solar radii) while traversing its atmosphere or corona as shown in Figure 1 to make fundamental observations of the least understood environment in the solar system [1, 2].

The spacecraft configuration is shown in Figure 2 with the large thermal shield dominating the configuration. The shield is a section of a parabola of revolution (paraboloid) which has a dual function as a shield and as a high gain antenna [3 - 7].

Measurements of the plasma environment including the birth and acceleration of the solar wind are the principal scientific objectives of this mission. To accomplish these measurements the spacecraft must not produce excessive outgassing or sublimation that could ionize and contaminate the natural plasma environments that are to be measured. The scientific community has suggested the magnitude of contamination that is acceptable and has given a total mass loss specification of less than 2.5 milligrams per second at perihelion.

Traveling to a perihelion radius of four solar radii ($4R_s$) requires a very high energy launch capability. In order to maximize the launch capability and minimize launch costs, the spacecraft must be as small and lightweight as possible while satisfying the scientific payload accommodation requirements. Thus, the shield must be made of lightweight materials such as composites. In addition, for a spacecraft traveling to $4R_s$ and maintaining its electronics at room temperature (approximately 300 K) a shield is required to shade the electronics while the shield itself will be operating at extremely high temperatures (greater than 2000 K). The combination of these requirements led to the selection of carbon-carbon as the ideal shield material because of its low density, high strength, and excellent high temperature characteristics. Carbon-carbon was also chosen because of its extensive recent history of development and its well known mechanical and thermal conductance properties. The only properties that are not as well known at high temperatures are the thermal-optical, radio reflectivity, and mass loss properties of its surface. These are the properties that are very important to the Solar Probe mission. Thus, the key challenge of this development was to determine these properties at the extreme solar fluxes and temperatures expected at perihelion. In addition, the design of the shield configuration for modal performance, stress analysis, and thermal analysis will be summarized.

2. HISTORY OF THE SHIELD CONCEPT

The history of the shield development is shown graphically by the spacecraft drawings in Figure 3. The early concepts for the Solar Probe (aka STARPROBE) utilized a large conical shield and a separate high gain antenna located below the shield in the shadow (or "umbra") of the shield. These concepts are shown in the panels "a" and "b" of the figure. Two architectural characteristics are illustrated in this figure. First, the early "STARPROBE" mission did not have a quadrature geometry at perihelion and the antenna boresight was about 45 degrees from the axis of the spacecraft as shown in panel "a" of the figure. As the mission evolved, the mission design changed to allow a quadrature trajectory at perihelion (sun-spacecraft-earth angle exactly 90 degrees). The first quadrature mission was introduced in 1989 and the boresight was then perpendicular to the axis as shown in panel "b". It then became apparent that if the shield were an off axis parabola, it could function as both a shield and an antenna. The result was that the large volume in the umbra necessary for the antenna could be eliminated. In 1992 a combined shield/antenna was first conceived and a dramatic change in the spacecraft architecture resulted as shown by the smaller spacecraft in panel "c". The diameter of the spacecraft was reduced from about 4 meters to about 1 meter with a correspondingly significant reduction in the mass of the spacecraft.

This shield/antenna concept has been the baseline for the Solar Probe since then and the current configuration is shown, for comparison, in panel "d" of Figure 3. This is a side view of the configuration in Figure 2.

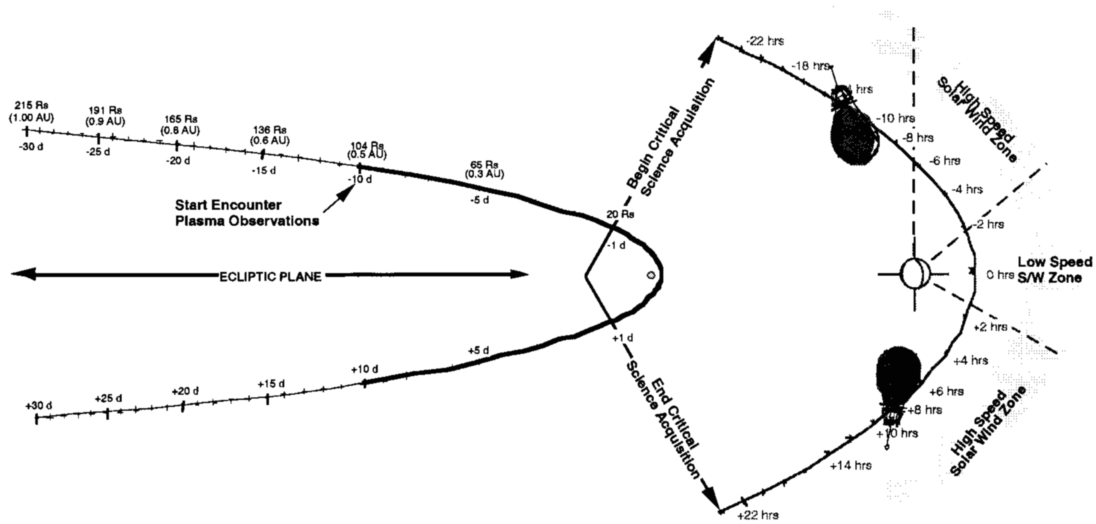

Figure 1. Solar Probe Perihelion Mission Profile as Seen from Earth

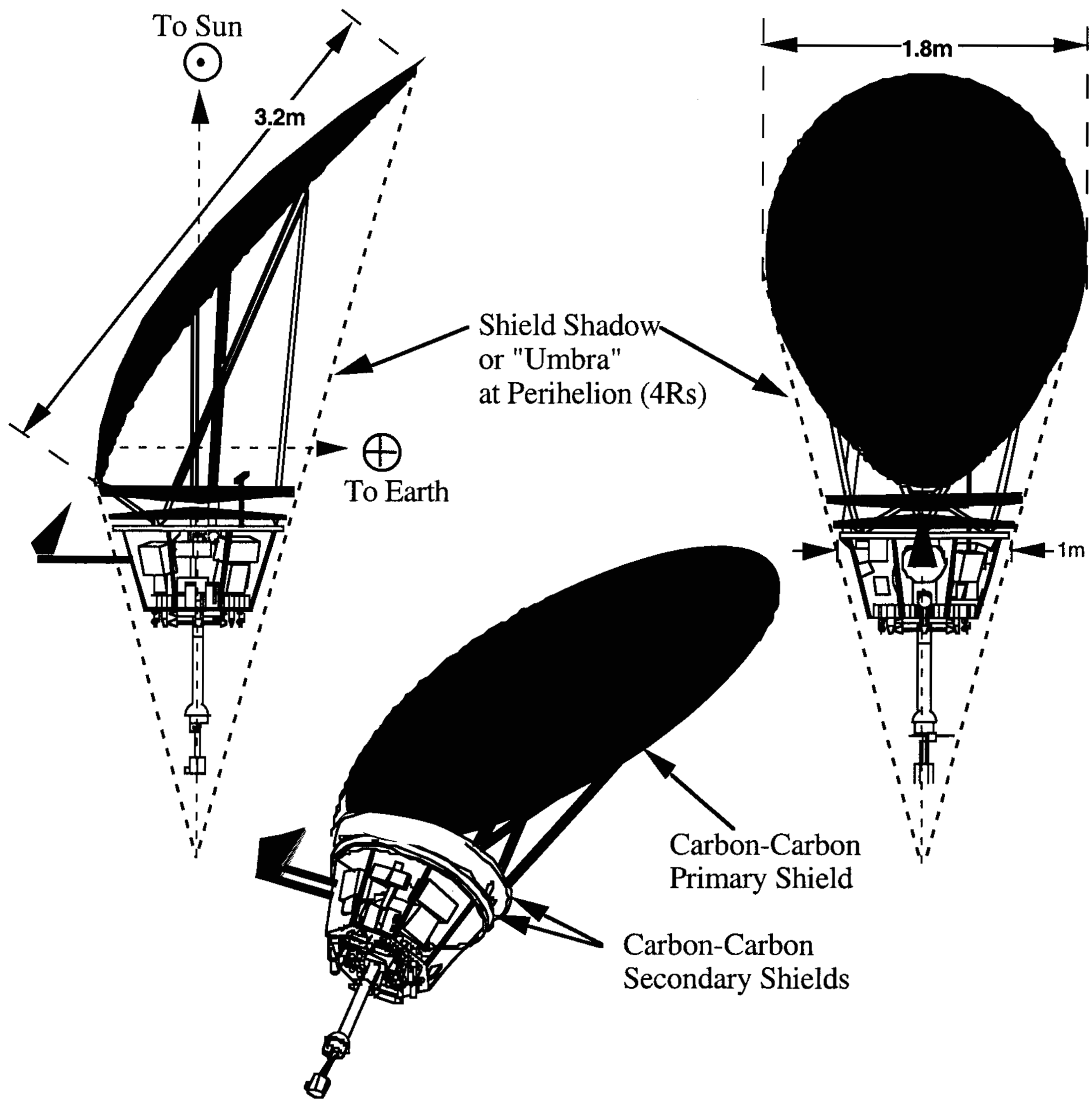

Figure 2. The Solar Probe Configuration at Perihelion

3. MATERIALS SELECTION

In an effort to understand the relationship between its thermal, mechanical, optical, and mass loss properties an extensive fabrication and testing program was conceived that would provide an empirical data for the utilization of Carbon-Carbon for this application. This program allowed a shield design that is predicted to function well in the extreme environment of the Solar Probe mission even though full scale testing of the shield in its thermal environment will not be possible. The inability to reproduce the perihelion flux environment in full scale testing has led to an extensive program to reduce risk and assure the understanding of the C-C materials properties by testing at the coupon level. The test specimens were fabricated using various techniques to identify how the fabrication techniques would affect the final carbon-carbon characteristics. Six specimens from

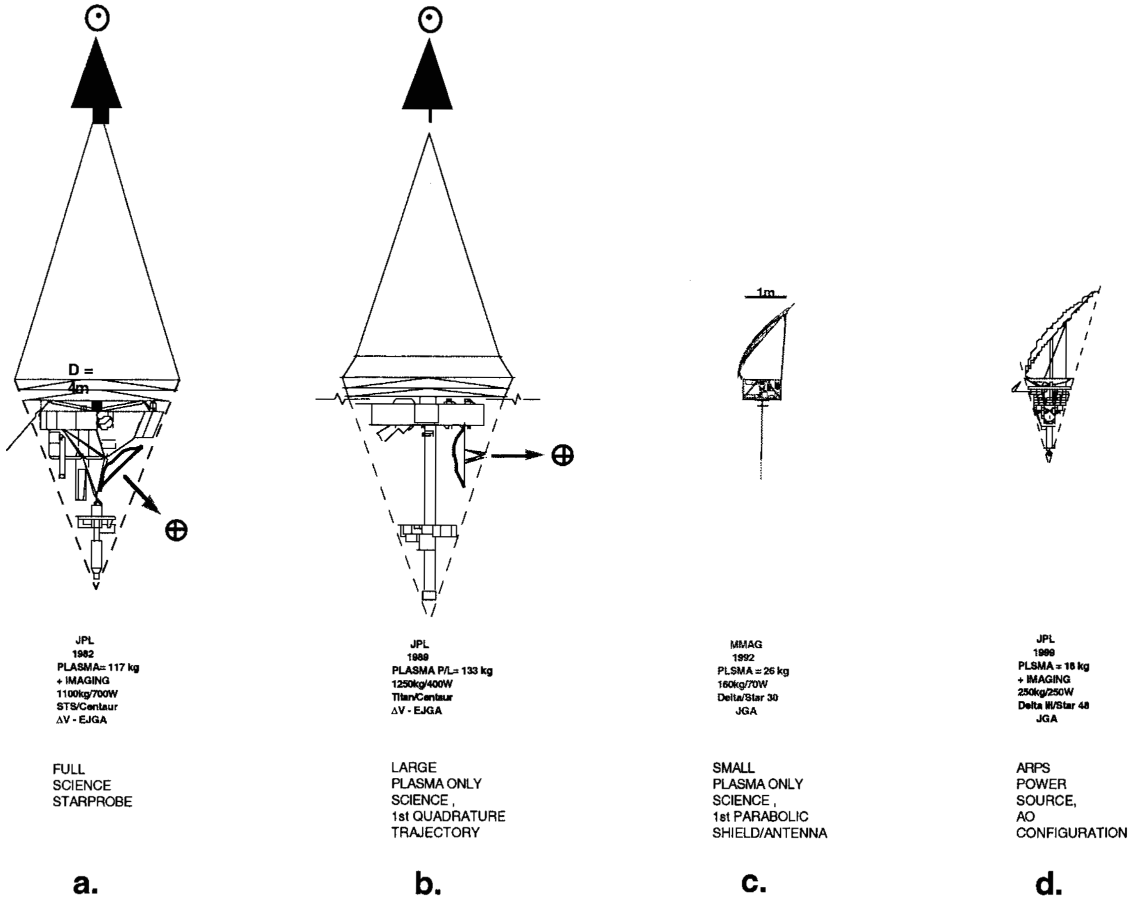

Figure 3. Shield Development History

four companies were tested. These samples varied in fiber, tow size, weave geometry, starting resin, and densification technique. The fabrication characteristics of the samples are summarized in Table 1. It was expected that the thermal-optical properties would depend on the final densification technique. Three techniques wee used as shown in the table: phenolic densification, chemical vapor infiltration (CVI), and pitch densification. It was expected that the CVI technique would be important but the other techniques were also studied. Thus, four of the six samples used CVI densification in addition to variations in fiber, tow size, prepregnation technique, and weave as shown in Table 1.

Table 1. Carbon-Carbon Test Samples

Coupon Number	Firm[1]	Fiber (Pitch Precursor)	Tow Size	Prepreg	Densification	Weave	Max Temp °C	Density g/cc
1	C-CAT	P-100	2K	Phenolic	Phenolic	8 HS	1700	1.68
2	BFG-1	K-321	2K	Hi-K	CVI	5 HS	2700	1.80
3	BFG-4	P-30	2K	Phenolic	CVI	5 HS	2700	1.79
4	BFG-5	K-321	4K	Phenolic	CVI	Tape	2700	1.75
5	FMI	P-55	2K	Pitch	Pitch	8 HS	2500	1.83
6	SAIC	T-300 HT (PAN Precursor)	3K	Phenolic	CVI + Sealcoat	8 HS	2200	1.49

1 C-CAT = Carbon-Carbon Advanced Technologies, Inc.; BFG = B. F. Goodrich; FMI = Fiber Materials Inc.; SAIC = Science Applications International Corp.

4. TESTING FACILITIES FOR SHIELD SAMPLES

Testing materials for the Solar Probe shield presents many facility challenges. The generation of almost 3000 Earth suns intensity (400 W/cm^2) in a space vacuum environment has required extensive facility development. A testing program [9] was initiated with Lockheed Martin Astronautics, (LMA, Denver, Colorado) to determine the thermal-optical properties of the carbon-carbon samples discussed above. Two test facilities were used for the thermal optical properties testing under the LMA program. A laboratory at LMA uses a high intensity ("VORTEK") halogen lamp beam that passes through a window into a vacuum chamber containing the sample. As the beam intensity was increased, the increasing temperature of the sample was measured for various angles of incidence by contact thermocouples. Figure 4 is a schematic image of the LMA facility. Knowing the flux input (I), the test data allows the direct determination of the ratio of solar absorptance (α) to hemispherical infrared emittance (ε) using the classical equation shown in Figure 4. Thus, by measuring the I and T values, the α/ε ratio can be determined in a well calibrated environment. In a separate facility at the Thermal Properties Research Laboratory (TPRL), West La Fayette, Indiana, the emittance for the same material was determined independently [9] in a laboratory that precisely measures hemispherical emittance using Joule heating of the sample.

5. MATERIALS TESTING RESULTS AND DISCUSSION

The fabrication process that affected the materials to the greatest extent was the final densification. Chemical Vapor Infiltration (CVI), as the final densification process, led to the most desirable thermal-optical properties. The most significant trend was a lower α/ε ratio at higher temperatures for the CVI densified materials. The other materials demonstrated a higher value of this ratio at higher temperatures. In addition to the CVI densification, the results suggest that a final seal coat of pyrolytic graphite (using carbon vapor deposition) lowers the α/ε ratio at high temperatures.

Figure 5 illustrates some of the emittance data from the TPRL testing for each of the samples shown. Note the similarity of the three samples (BFG-1, BFG-4, and C-CAT) and the significantly higher emittance in the FMI sample. The FMI sample was pitch densified and suggested, early in the program, that this technique produced a unique emittance result. The data of the LMA measurements using the VORTEK facility are shown in Figure 6. These results include the determination of the temperatures of the samples and the calculation of the α/ε ratio using the equation in Figure 4. Note that the BFG-5 and the SAIC sample data suggests a nearly flat or even decreasing α/ε as temperature increases. The FMI sample, which had such a high emittance (Figure 5) at high temperatures, also has the highest α/ε ratio at high temperatures.

The emittance of optically opaque materials such as graphite depends on both the chemical composition and the geometrical structure of the surface. Recent data from Neuer [10] shows a decrease in the spectral emittance of graphite with increasing wavelength from 0.65 to 6 microns. This spectral behavior would tend to increase emittance with temperature as shown in Figure 5 as the blackbody emission spectrum shifts to shorter wavelengths at higher temperatures. There may also be an effect of the degree and extent of crystallinity of the graphitic structure. Data reported by Kelly [11] indicates that the spectral emittance of the basal planes of graphite crystals is lower than that perpendicular to them. Neuer [10] also noted that the emittance of carbon fibers is relatively low and this may be due to their oriented graphitic nature. Because CVD densification produces the most graphitic and largest scale of oriented graphitic structure, the emittance of CVD materials would be expected to be lower than that of pitch and resin processed materials.

Surface geometrical effects may also be contributing to the observed test results. Neuer [10] points out that the emittance of the planar surface of 2D woven fabric composites may be dominated by the surface characteristics of the fibers and roughness/porosity effects. Kelly [11] also noted that the emittance of rough surfaces is higher than that of smooth surfaces perhaps due the surface pores acting as “small black body cavities”. Both the pores at the surface and the “grooves” between the fibers may contribute to this cavity effect that increases the emittance. Since typical fiber diameters are between 7 and 12 microns and surface pores in CVD processed materials are of similar size, the effect is limited to short wavelengths and could be especially important in the solar radiation spectrum. Surface pores in pitch processed materials tend to be larger and may produce the higher emittance measured for the FMI material.

Based on these observations, the α/ε ratio for smooth graphitic surfaces would be expected to decrease with increasing temperature as illustrated by the data trends in Figure 6. However, surface roughness may tend to increase the effective emittance especially at the shorter wavelengths thereby increasing α, and α/ε may either remain constant or increase with temperature. The smoothest material, the SAIC seal coated material, exhibited a decrease in α/ε with increasing temperature. The BFG-4 tape material, which would be expected to be almost as smooth as the SAIC material, showed little change in α/ε with temperature. The other materials all exhibited increases in α/ε with increasing temperature and the FMI material (that may have been the roughest material due to both the pitch process and machining) showed the greatest increase with temperature.

These results suggest some significant trends that depend on the fabrication processes although the data is quite sparse. If these trends are correct, the combination of phenolic pre-pregnation and CVI final densification suggests that the α/ε ratio is nearly a constant (or decreasing) function as temperature increases. This is very desirable for the Solar Probe to minimize the shield temperatures (and mass loss) at the high solar flux at perihelion. The solar absorptance (α) was not measured directly but can be inferred from the TPRL results and the LMA results. The "I" and "F" values shown on the right axis of Figure 6 refer to the initial (I) shield design value prior to the test program and the final (F) suggested value as a result of the tests.

The mass loss from the samples was measured in a special furnace facility [9] that heated the samples over progressively longer durations while the mass of the samples was measured precisely between each heating interval. Thermal-mechanical properties were measured using standard techniques at the NASA Langley Research Center and its contractors [8]. The test results suggest some consistent trends. The materials that had CVI densification also exhibited the highest values of elastic modulus and mechanical strength. Radio reflectivity tests [12] were run on the materials and they demonstrated reflectivity suitable for an antenna reflector at the X-band frequencies to be used on the Solar Probe. Reflectivity losses of less than 0.1 dB at temperatures about 1500 K were determined.

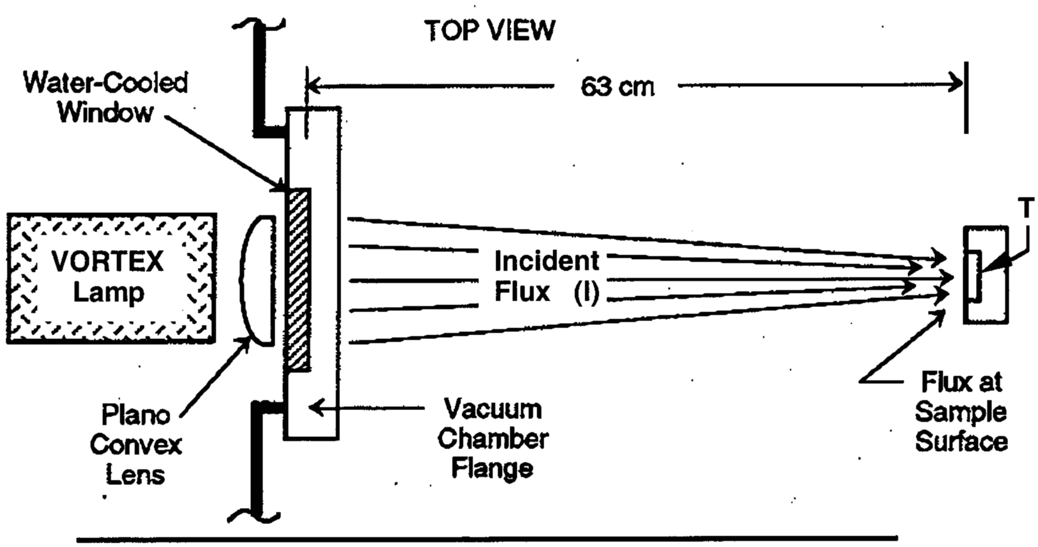

$\alpha_S / \varepsilon_h = \sigma T^4 / I$

α_S = Solar Absorptance / ε_h = Hemispherical Emittance
σ = Stephan-Boltzmann constant
T = Temperature
I = Incident Flux (from VORTEX)

Figure 4. Schematic Drawing of LMA VORTEK Testing Facility and Analytical Solution for α/ε

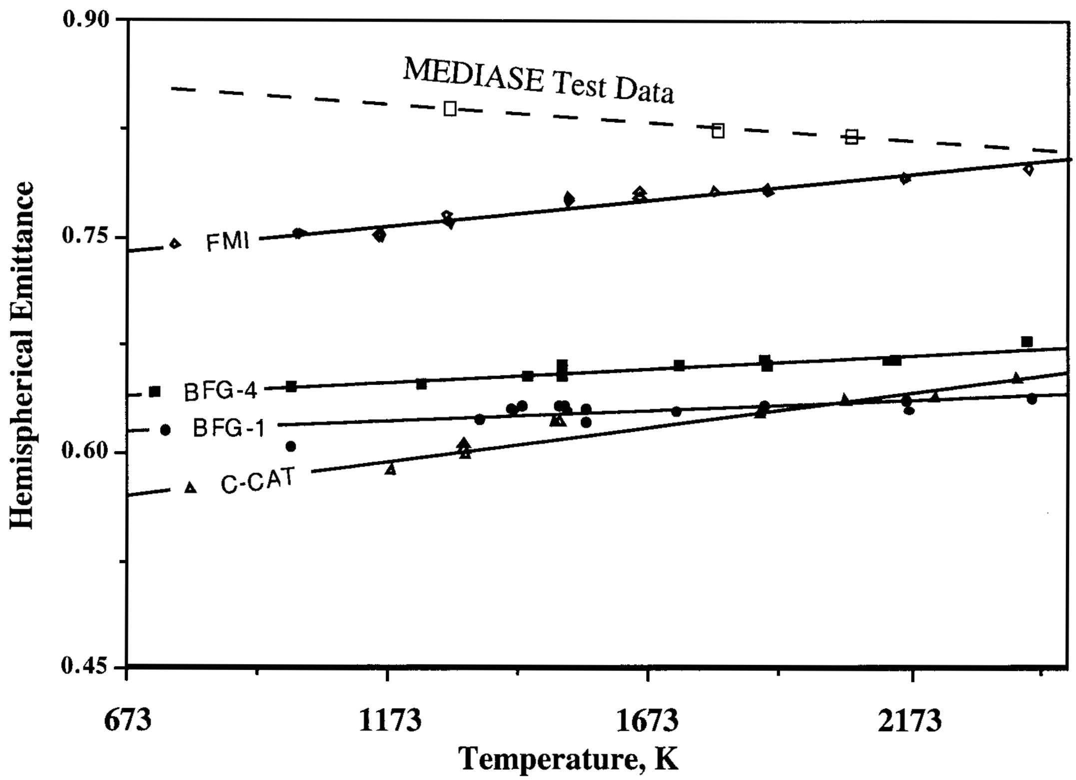

Figure 5. Emittance of Selected Samples vs. Temperature

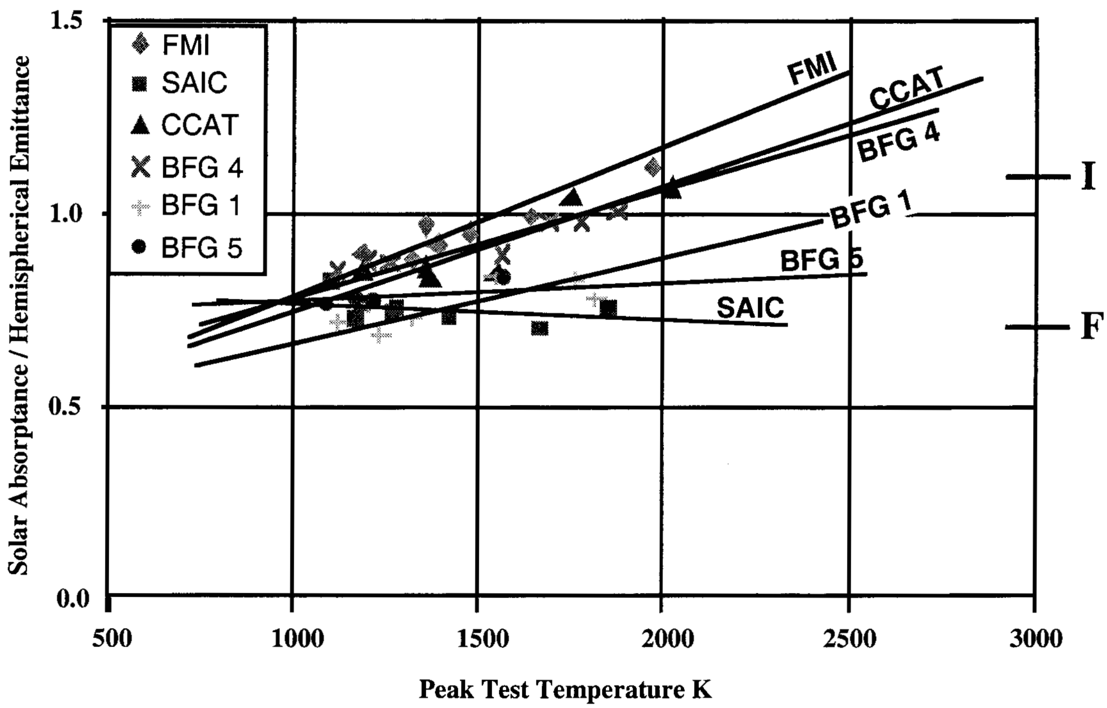

Figure 6. Ratio of Solar Absorptance to Hemispherical Emittance vs. Temperature for the U.S. Test Samples (zero degrees incidence angle)

The test results for the thermal-optical properties suggest that a shield fabricated from a carbon-carbon material that uses a phenolic pre-pregnation and a CVI final densification will perform well at perihelion. The new results allow the determination of a design space for the Solar Probe shield as shown in Figure 7. Here the shield temperature and mass loss are plotted versus the α/ε ratio. The preliminary mass loss requirement specified by the science team [1] is less that 2.5 mg/sec at perihelion and is the key design parameter. Prior to the testing program the α/ε design value of the carbon-carbon was assumed to be 1.1. As can be seen from Figure 7, the peak shield temperature (~ 2350 K) and the mass loss (~0.6 mg/sec) are below the requirement for this α/ε ratio. If the material has the properties of the CVI densified sample, or α/ε = 0.7, as shown in Figure 7, the temperature and mass loss would drop significantly to ~ 2100 K and ~ 0.006 mg/sec. This drop of almost two orders of magnitude in mass loss suggests that the contamination of the scientific measurements by the spacecraft shield sublimation is no longer a concern.

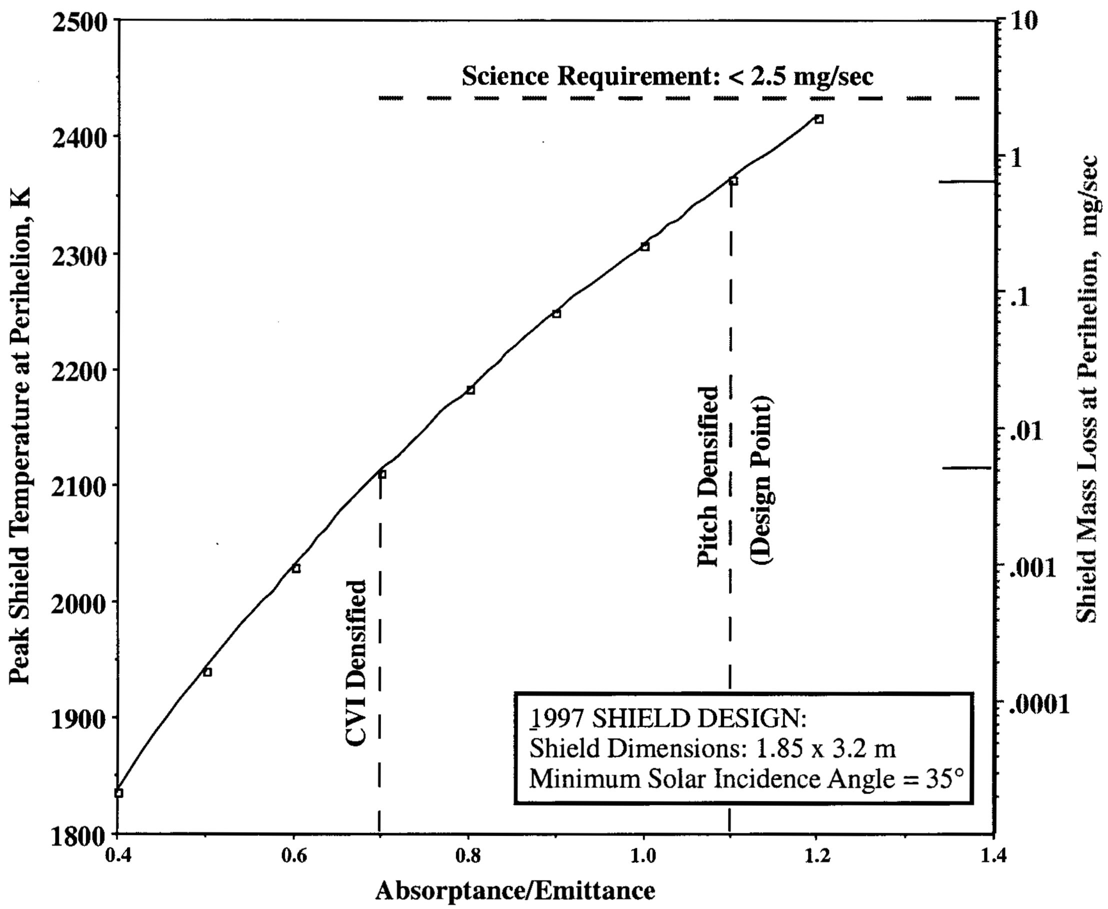

Figure 7. Shield Peak Temperature and Mass Loss vs. a/e ratio

ACKNOWLEDGEMENTS

The research described in this paper was carried out at the Jet Propulsion Laboratory, California Institute of Technology, under a contract with the National Aeronautics and Space Administration.

REFERENCES

[1] Randolph J, Ayon J, Leschly K, Miyake R, Tsurutani B. International Symposium on Optical Science, Engineering, and Instrumentation: SPIE, 1998; 3442-02.

[2] Randolph J, Ayon J, Harvey G, Imbriale W, Miyake R, Mueller R, Nesmith B, Turner P, Dirling R, Rawal S, Vaughn W. American Institute of Physics Proceedings, 1997; 387: 123.

[3] Millard JM, Maag CR, Miyake RN. AIAA Progress in Astronautics and Aeronautics: AIAA, 1983; 85: 351.

[4] Millard JM, Miyake RN, Dirling RB, Rolfo A, Royere C. ESA SP-200, 1983:531

[5] Miyake RN, Millard JM, Randolph JE. AIAA 26th Thermophysics Conference: AIAA, 1991; 91-1319.

[6] Millard JM, Miyake RN, Rainen RA. AIAA 30th Aerospace Sciences Meeting: AIAA, 1992; 92-0862.

[7] Randolph J. NASA Tech Briefs NPO-20318, 1998.

[8] Vaughn WL, Ransome PO, Sienko KH. 21st Annual Conference on Composites, Materials and Structures of the U. S. Advanced Ceramic Association, 1997; 717.

[9] Rawal S, Pierson E, Valentine P, Trester P, Harrington R, Taylor R. Final Contract Report for JPL, Lockheed Martin Astronautics MCR-97-594, 1997.

[10] Neuer G. High Temperature-High Pressures 1995/1996; 27/28: 183.

[11] Kelly BT. Physics of Graphite; Applied Science, 1981: 317.

[12] Pierson, E, Milligan, T. Final Contract Report for JPL, Lockheed Martin Space Systems - Astronautics, MCR - 99 - 522